Dehydrated Human Amniotic Membrane Inhibits Myofibroblast Contraction through the Regulation of the TGFβ–SMAD Pathway In Vitro

Sarah E. Moreno[1], Michelle Massee[1] and Thomas J. Koob[1]

Excessive fibrosis affects more than 100 million patients yearly, leading to the accumulation of extracellular matrix that compromises tissue architecture and impedes its function. Intrinsic properties of the amniotic membrane have alluded to its potential to inhibit excessive fibrosis; therefore, this study aimed to investigate the effects of dehydrated human amnion/chorion membrane (dHACM) on dermal fibroblasts and their role in fibrotic pathways. Human dermal fibroblasts were stimulated with TGFβ1, triggering myofibroblast-like characteristics in vitro. Subsequent addition of dHACM in the continued presence of TGFβ1 inhibited downstream signaling, leading to a reduction in the expression of known fibrotic and extracellular matrix genes. In addition, dHACM decreased alpha-smooth muscle actin, a stress filament responsible for contractile activity in scarring. The functional outcome of these effects was observed in an ex vivo model for cellular contraction. Hyperactivation of TGFβ signaling increased the contractile capacity of myofibroblasts embedded within a collagen substrate. Simultaneous addition of dHACM treatment prevented the marked contraction, which is likely a direct result of the inhibition of TGFβ signaling mentioned earlier. These observations may support the use of dHACM in the regulation of fibroblast activity as it relates to tissue fibrosis.

JID Innovations (2021);**1:**100020 doi:10.1016/j.xjidi.2021.100020

INTRODUCTION

Fibrosis or the de novo production of a fibrous extracellular matrix (ECM) is a necessary phase of the normal healing cascade, providing the provisional matrix required to restore tissue function. During the normal healing process, inflammatory cells and the resident cell population release chemotactic signals, activating fibroblastic cells to migrate into the damaged tissue. Subsequent release of profibrotic factors from these cells stimulates fibroblast differentiation into myofibroblasts. Myofibroblasts are responsible for synthesizing the ECM components as well as for facilitating wound contraction through the development of intracellular microfilament stress fibers. As the remodeling phase of healing commences, a feedback mechanism triggers myofibroblast apoptosis to eliminate this contractile, profibrotic cell type from the newly epithelialized tissue, returning to a state of homeostasis and initiating tissue maturation (El Ayadi et al., 2020). The resultant tissue is remodeled over time, restoring it to near-normal tissue architecture and mechanical strength with minimal long-term complications.

Pathologic processes, such as chronic inflammation, persistent myofibroblast activation, and unabated fibroblast proliferation, coupled with ECM deposition, can disrupt the normal healing cascade and promote the development of excessive fibrosis (El Ayadi et al., 2020; Wynn, 2008). Depending on the severity of the underlying condition, pathologic fibrosis complications may range from visibly disfiguring dermal scarring, limiting the full range of motion in the affected tissue, as in keloid and hypertrophic scarring, to propagating fibrosis, impairing vital organ function, as in the case of pulmonary and liver fibrosis (Marshall et al., 2018). The number of patients affected by fibrotic complications is widespread across a multitude of conditions, including infections, autoimmune reactions, toxins, radiation, mechanical injuries such as severe burns, trauma, or surgical incisions (Wynn, 2008). As a result, the magnitude of this affliction is significant. Reports show that the incidence of forming hypertrophic scars alone ranges from 40% to 70% after surgery and up to 91% after burn injury (Gauglitz et al., 2011).

Although the initiating events leading to pathologic scar formation arise from varying etiologies, recent advances have identified key, universal effector cells and molecular regulators common to most scar pathologies (El Ayadi et al., 2020). In most instances, the cells and mediators involved in aberrant fibrosis are also critical for normal processes. However, the elevated and/or sustained presence of these targets is responsible for excessive fibrosis. TGFβ1 is considered a key molecule in the activation of the fibrotic process, targeting fibroblasts, a key cell type in the fibrotic process. TGFβ signaling predominately mediates intracellular activity through the SMAD signaling pathway. The binding of the ligand constitutively phosphorylates the receptor complex

[1]*MiMedx Group, Inc, Marietta, Georgia, USA*

Correspondence: Michelle Massee, Research and Development, MiMedx Group, Inc, 1775 West Oak Commons Court Northeast, Marietta, Georgia 30062, USA. E-mail: mmassee@mimedx.com

Abbreviations: dHACM, dehydrated amnion/chorion membrane; ECM, extracellular matrix; FN, fibronectin; HDF, human dermal fibroblast; αSMA, alpha-smooth muscle actin

Received 10 February 2021; revised 31 March 2021; accepted 8 April 2021; accepted manuscript published online 6 May 2021; corrected proof published online 31 May 2021

Cite this article as: JID Innovations 2021;1:100020

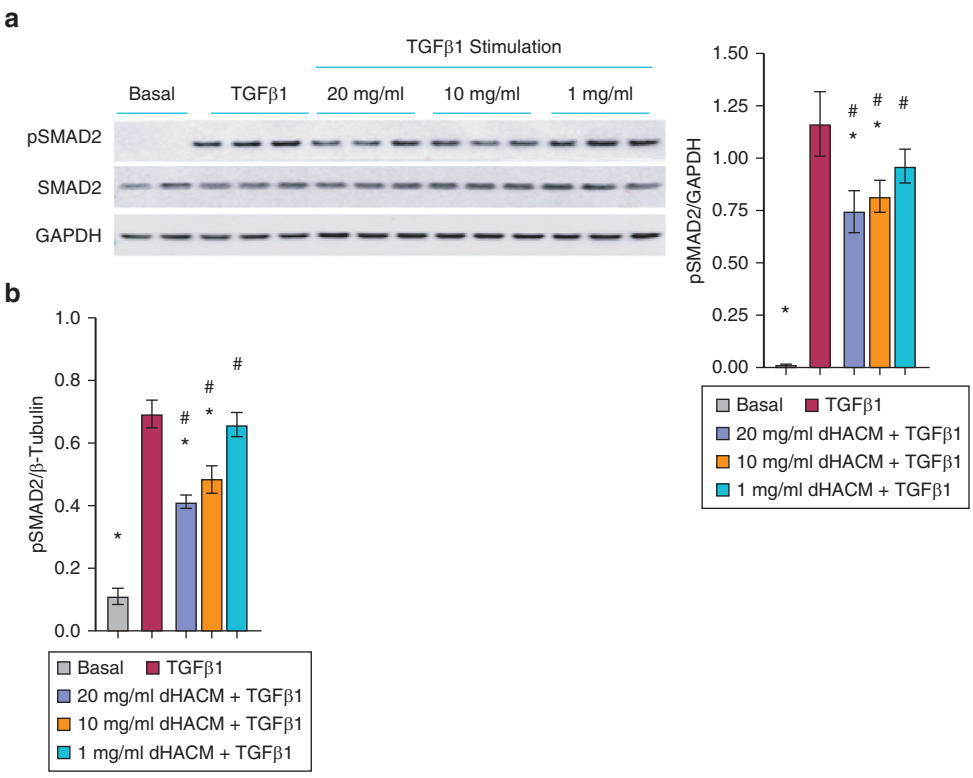

Figure 1. dHACM treatment inhibits the phosphorylation of SMAD2 in cultured HDFs. Normal HDFs were stimulated with 20 ng/ml TGFβ1 for 24 hours followed by treatment with dHACM at 20, 10, or 1 mg/ml for 24 hours. Phosphorylation of SMAD2 in the fibroblasts was assessed by (**a**) western blot and (**b**) Luminex analysis. Values are normalized relative to those of the endogenous control for each experiment. All values represent mean ± SD. *$P < 0.05$ versus TGFβ1 group and #$P < 0.05$ versus basal group using one-way ANOVA; n = 3 dHACM donors. dHACM, dehydrated human amnion/chorion membrane; HDF, human dermal fibroblast; pSMAD2, phosphorylated SMAD2.

and induces intracellular signaling by the SMAD2 and SMAD3 transcription factors that regulate the expression of several fibrotic genes, including CTGF; fibronectin (FN); alpha-smooth muscle actin (αSMA); and ECM components, including type I collagen (Walton et al., 2017). TGFβ signaling provides a signal to drive the differentiation of fibroblasts into myofibroblasts. Hyperactivation of TGFβ results in the prolonged presence of myofibroblasts, which is responsible for the continuous secretion of ECM components and increased contractile capacity, all leading to abnormal tissue architecture and excessive scarring (Walton et al., 2017).

Modulation of myofibroblasts is a promising therapeutic concept for targeting new drug development to reduce pathologic scarring (Van De Water et al., 2013; Yazdani et al., 2017). Dehydrated human amnion/chorion membrane (dHACM) (MiMedx Group, Marietta, GA) is a PURION-processed amniotic membrane allograft. Previous studies have shown that this proprietary process retains well-known regulatory proteins inherent to amniotic tissues and preserves the bioactivity to stimulate cellular activities, such as proliferation, migration, and biosynthesis in multiple cell types (Koob et al., 2014a; Koob et al., 2014b; Koob et al., 2013; Lei et al., 2017; Massee et al., 2016a; Massee et al., 2016b). Clinical studies showed efficacy in diseases with varying etiologies, ranging from chronic wounds to musculoskeletal injuries to pediatric burns, suggesting that the complex nature of dHACM may prove useful in a multitude of applications where normal healing is impaired (Ahuja et al., 2020; Cazzell et al., 2018; Fetterolf and Snyder, 2012; Patel et al., 2015; Price and Price, 2016; Serena et al., 2014; Zelen et al., 2013).

In this study, an in vitro system was developed to evaluate the effect of dHACM on human dermal fibroblasts (HDFs) activated by sustained treatment with TGFβ1. It is hypothesized that dHACM disrupts the TGFβ signaling pathway, leading to a reduced contractile phenotype through the decreased expression of fibrotic factors and ECM components and reduced differentiation of myofibroblasts. This proposed mechanism may translate to an effective therapy to improve outcomes from injuries where regulation of fibroblast activity may lead to improved outcomes.

RESULTS

dHACM antagonizes the phosphorylation of SMAD2 in cultured HDFs

Dysregulation of the TGFβ–SMAD pathway is an important pathogenic mechanism contributing to the imbalance in ECM deposition and the degradation seen in fibrotic diseases (Walton et al., 2017). In vitro stimulation of HDFs with recombinant TGFβ1 increased the expression of phosphorylated SMAD2 (Figure 1). Protein analysis of the phosphorylation status of SMAD2 by western blot and Luminex analysis demonstrated that dHACM significantly attenuated the TGFβ1-induced phosphorylation of SMAD2 without affecting total SMAD2 expression (Figure 1a and b).

dHACM inhibits TGFβ1-induced fibrotic responses in cultured HDFs

To understand the effects of dHACM on the TGFβ1-induced fibrotic response, HDFs were stimulated with TGFβ1 for 24 hours followed by 24-hour treatment with dHACM in the presence of TGFβ1. As shown in Figure 2a and b, recombinant TGFβ1 stimulated an increase in mRNA expression of fibrotic markers *PAI-1* and *CTGF*. A 24-hour treatment with

20 and 10 mg/ml of dHACM + TGFβ1 significantly suppressed the TGFβ1-dependent induction of both mRNAs to similar levels seen in the basal control. Treatment at 1 mg/ml dHACM + TGFβ1 affected CTGF expression; however, it increased the expression of PAI-1 compared with that of TGFβ1 alone.

The biologic effects of dHACM on in vitro ECM synthesis were evaluated. A comparison of the control groups demonstrated that HDFs stimulated with TGFβ1 resulted in increased gene expression of ECM components *COL1A1*, *FN1*, and *ELN* compared with that of unstimulated control (basal) (Figure 2c, e, and f). No change was observed in *COL3A1* on TGFβ1 stimulation (Figure 2d). *COL1A1* and *FN1* expression was significantly reduced by treatment with 20 and 10 mg/ml of dHACM + TGFβ1, whereas the expression of *ELN* was reduced with 20, 10, and 1 mg/ml dHACM + TGFβ1.

dHACM attenuates TGFβ1-mediated myofibroblast differentiation

TGFβ governs the differentiation of fibroblasts to myofibroblasts, resulting in increased synthesis of αSMA (Vallée and Lecarpentier, 2019). Fibroblasts stimulated with 20 ng/ml of TGFβ1 showed increased mRNA expression of *αSMA* compared with that of unstimulated control (basal) in this model (Figure 3a). Treatment with 20, 10, or 1 mg/ml dHACM significantly suppressed the TGFβ1-dependent induction of the *αSMA* mRNA in a dose-dependent manner. Moreover, the TGFβ1-dependent increase of *αSMA* mRNA was decreased to the basal level at both the 20 and 10 mg/ml doses (Figure 3a).

The effect of dHACM on the protein expression of αSMA was evaluated using western blotting and immunofluorescence (Figure 3b and c). TGFβ1-induced protein expression of αSMA on HDFs was significantly inhibited by dHACM treatment at 20 and 10 mg/ml. There was no observable effect at 1 mg/ml (Figure 3b). In addition, immunofluorescence staining demonstrated that treatment with dHACM at 20 and 10 mg/ml inhibited the TGFβ1-induced αSMA expression in HDFs (Figure 3c).

Reduction in αSMA by dHACM contributes to the reduced contractile capacity of fibroblasts

Increased differentiation into myofibroblasts mediated by TGFβ1 leads to increased contractile properties of the fibroblast cells (Vallée and Lecarpentier, 2019). Fibroblasts were seeded in collagen gels followed by treatment with media alone (vehicle control), TGFβ1 concentration (positive control), or dHACM concentration in the presence of TGFβ1 (Figure 4). Gel diameter was measured 48 hours after the treatment. Fibroblasts treated with TGFβ1 contracted the surrounding matrix, leading to the contraction of the gel. dHACM at 20, 10, and 1 mg/ml attenuated the contraction by fibroblasts when combined with TGFβ1 (Figure 4a and b). The amount of contraction at the doses of 20 and 10 mg/ml dHACM was similar to that seen in the vehicle control in which there was minimal gel contraction, whereas treatment with 1 mg/ml, although significantly different from treatment with the positive control,

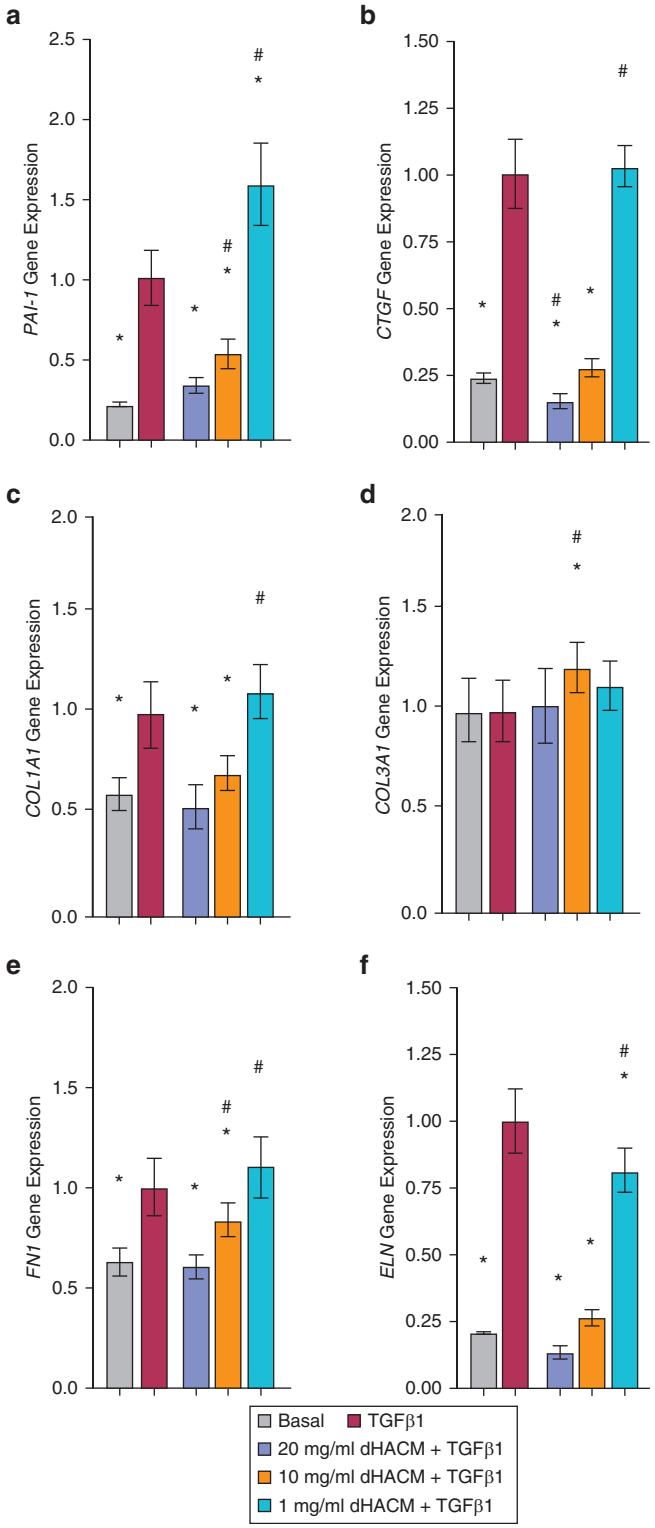

Figure 2. Effect of dHACM on TGFβ1-induced fibrotic response in HDFs. Fold change in gene expression of fibrosis markers (**a**) *PAI-1* and (**b**) *CTGF* and ECM components (**c**) *COL1A1*, (**d**) *COL3A1*, (**e**) *FN1*, and (**f**) *ELN* in HDFs after 24-hour stimulation with TGFβ1 and 24-hour treatment with dHACM + TGFβ1. Values are normalized relative to those of 18S endogenous control for each experiment. All values represent mean ± SD. *$P < 0.05$ versus TGFβ1 group and #$P < 0.05$ versus basal group using one-way ANOVA; n = 3 dHACM donors. dHACM, dehydrated human amnion/chorion membrane; ECM, extracellular matrix; ELN, elastin; FN, fibronectin; HDF, human dermal fibroblast.

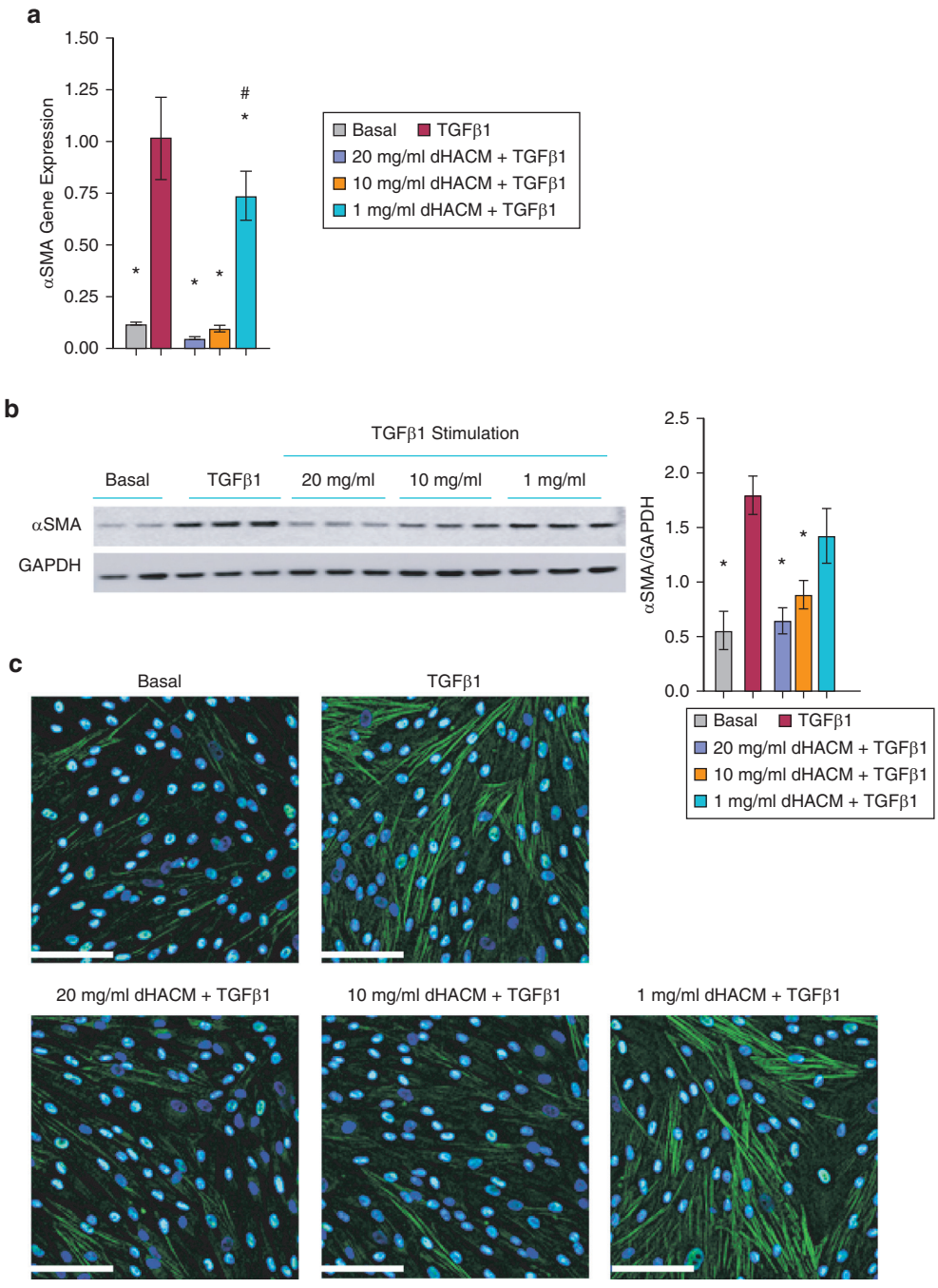

Figure 3. Effect of dHACM on TGFβ1-mediated αSMA synthesis. (**a**) mRNA level of *αSMA* in HDFs normalized to those of 18S and expressed as a fold change compared with that of TGFβ1. (**b**) Expression of αSMA in fibroblasts assessed by western blot analysis. All values represent mean ± SD. $*P < 0.05$ versus TGFβ1 group and $\#P < 0.05$ versus basal group using one-way ANOVA; n = 3 dHACM donors. (**c**) Representative IF staining for αSMA. Bar = 100 μm. dHACM, dehydrated human amnion/chorion membrane; HDF, human dermal fibroblast; IF, immunofluorescence; αSMA, alpha-smooth muscle actin.

did not prevent contraction to the level of the vehicle control (Figure 4b).

Immunofluorescence analysis of the collagen gels showed that the expression of αSMA in cells correlates with the contraction measurements in Figure 4b and c. As shown in the representative images, dHACM reduced the expression of αSMA induced by TGFβ1 to levels similar to what is seen in the unstimulated basal group (Figure 4c). No immunofluorescence signal was detected in isotype or secondary controls (Figure 5).

DISCUSSION

Complications arising from aberrant fibroblast activity after the abnormal repair of an injury may often result in pain and dysfunction. The fibrotic response is a normal phase of the healing process triggered by the TGFβ–SMAD signaling pathway. Activation of this pathway results in downstream signals that facilitate the differentiation of the resident fibroblasts into myofibroblasts. These cells function in the deposition of ECM components and exhibit a contractile phenotype to promote wound closure. However, when the

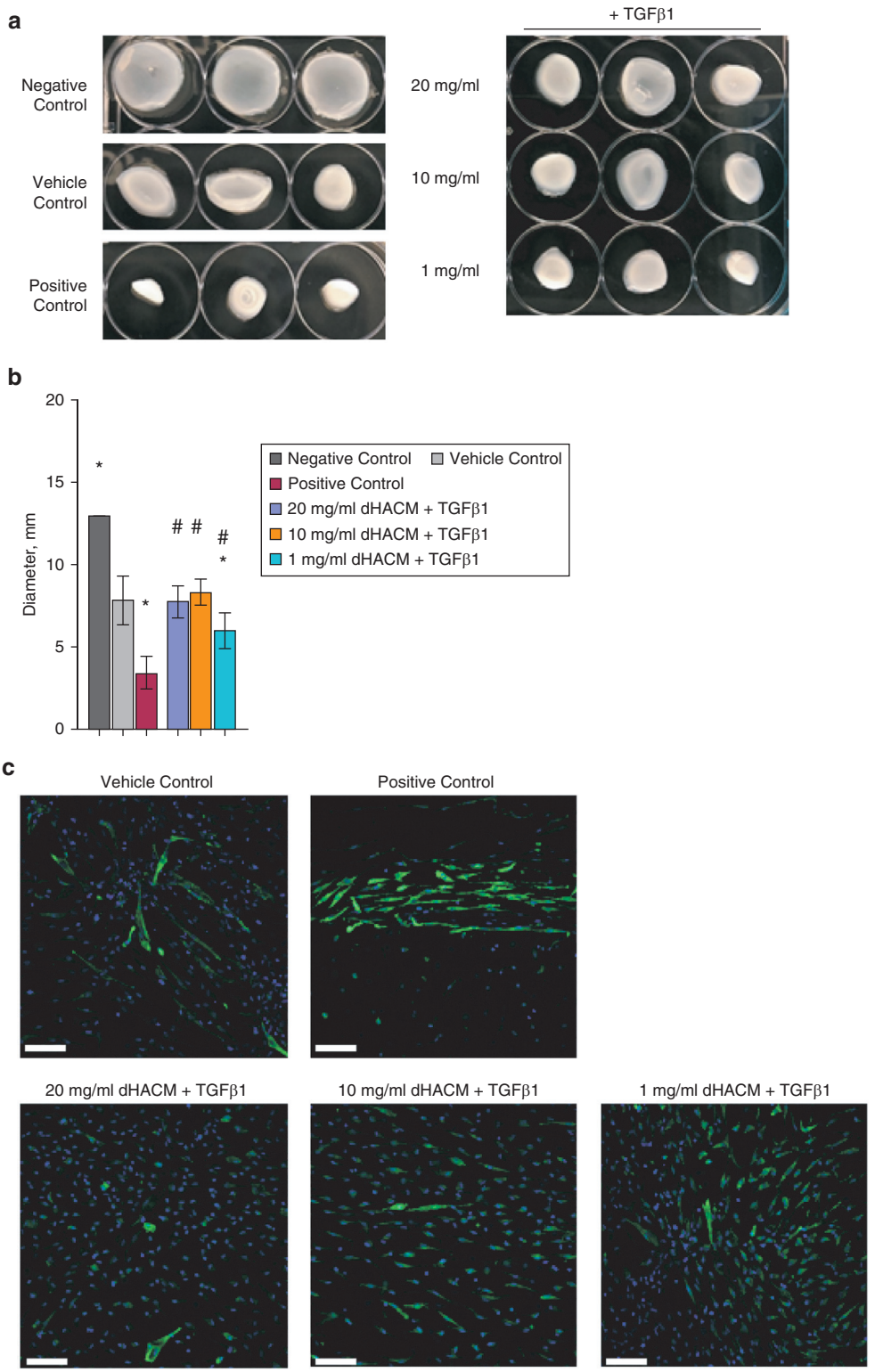

Figure 4. dHACM suppresses TGFβ1-stimulated contraction of fibroblasts. (**a**) Representative images of collagen gels. (**b**) After 48 hours, the diameter of each collagen gel was measured. Treatments include no cells (negative control), media alone (vehicle control), 20 ng/ml TGFβ1 (positive control), 20 mg/ml dHACM + 20 ng/ml TGFβ1, 10 mg/ml dHACM + 20 ng/ml TGFβ1, and 1 mg/ml dHACM + 20 ng/ml TGFβ1. All values represent mean ± SD. $*P < 0.05$ versus vehicle control and $\#P < 0.05$ versus positive control using one-way ANOVA; n = 3 dHACM donors. (**c**) Representative IF staining for αSMA. Bar = 100 μm. dHACM, dehydrated human amnion/chorion membrane; IF, immunofluorescence.

TGFβ signal continues unabated, the fibrotic response becomes pathologic (Frangogiannis, 2020). The resultant excessive scarring may be visibly disfiguring, which presents its own set of psychosocial issues, but the underlying impact on tissue structure is what ultimately leads to painful contractures and limited mobility and functionality (Brown et al., 2008). Identifying a treatment to regulate the pathways contributing to pathologic fibrosis would be a substantial benefit to not only the patient but also the healthcare providers because an efficacious, nonsurgical intervention is not currently available.

Since the discovery of scarless fetal skin wound healing, research efforts have attempted to recreate this finding in the adult population, including treatments comprising GFs, cytokines, and ECM substitutes. However, no individual

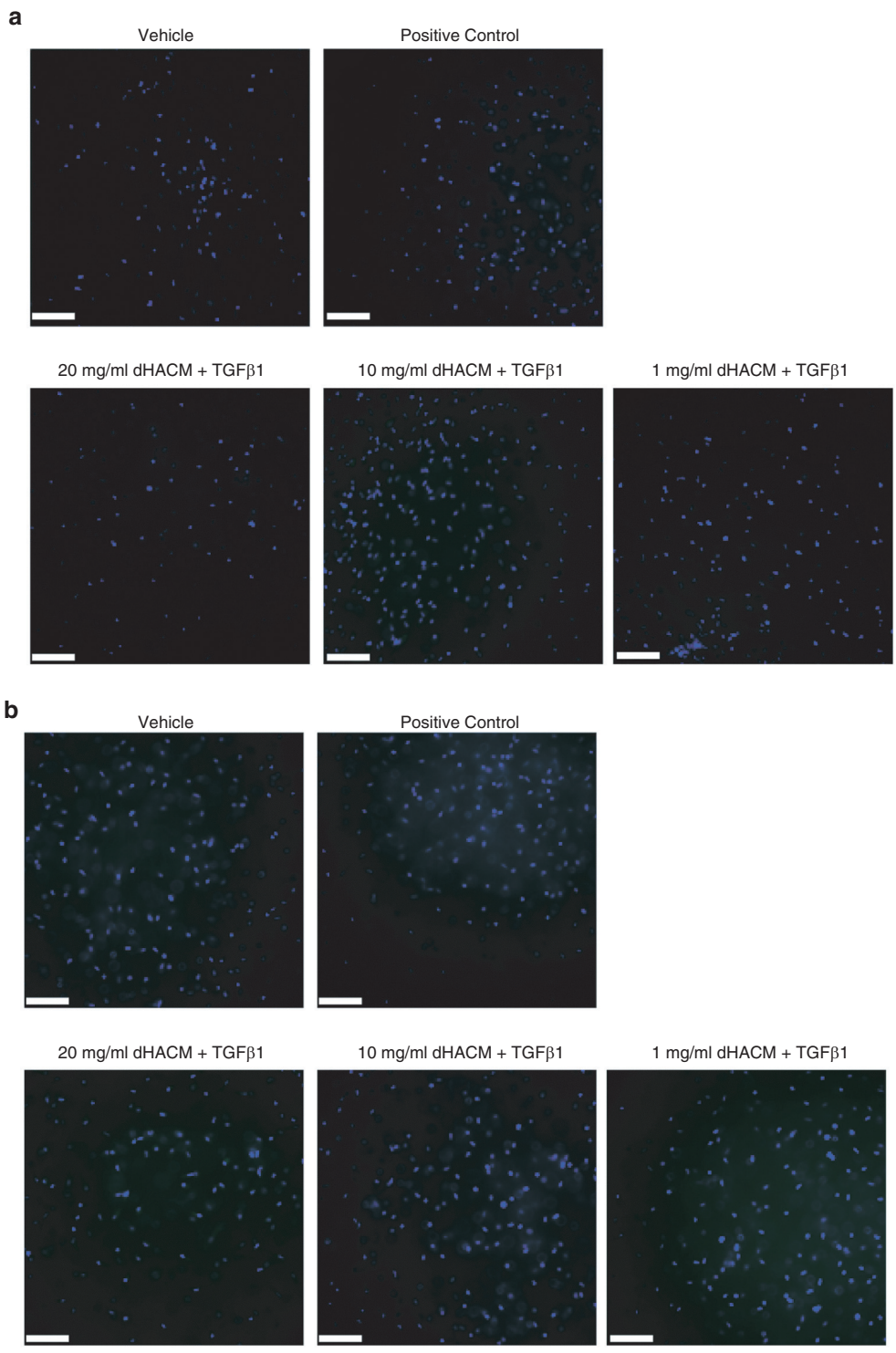

Figure 5. Control IF of collagen gels. Collagen gels treated with media alone (vehicle control), 20 ng/ml TGFβ1 (positive control), 20 mg/ml dHACM + 20 ng/ml TGFβ1, 10 mg/ml dHACM + 20 ng/ml TGFβ1, and 1 mg/ml dHACM + 20 ng/ml TGF-β1. Representative images of IF control staining using (**a**) mouse IgGa2a and (**b**) secondary antibody only. Bar = 100 μm. dHACM, dehydrated human amnion/chorion membrane; IF, immunofluorescence.

treatment, pathway, or cell subtype has proven sufficient to support scarless wound healing in adult skin (Moore et al., 2018). Although the role of the amniotic membrane in fetal scarless healing is not fully understood, it does play a critical role in maintaining the protective environment and supplying the amniotic fluid with signaling factors necessary to regulate developmental processes. Therefore, amniotic membrane allografts may best capture these properties and allow for large-scale application. Advanced biologic interventions, such as dHACM, may facilitate improved outcomes by regulating fibroblast activity, thereby promoting a normal healing response. The purpose of this study was to elucidate the potential mechanisms of action for the role of dHACM in the regulation of fundamental fibroblast activities related to fibrosis.

TGFβ regulates numerous intracellular signaling cascades to transmit its profibrotic effects; thus, inhibition of TGFβ signaling offers potential for antifibrotic therapies (Györfi et al.,

2018; Walton et al., 2017). Fibroblasts, challenged with TGFβ1, exhibited an upregulation of the SMAD signaling pathway and increased the expression of key genes associated with fibrosis, confirming the induction of a fibrotic environment in an in vitro model. The subsequent addition of dHACM treatment resulted in a significant reversal of the TGFβ1-induced changes. Decreases in phosphorylated SMAD2 signified that dHACM directly interrupted TGFβ signaling and decreased downstream gene regulation, including *αSMA*, *PAI-1*, and *CTGF*, all three of which contribute to the accumulation of collagen and reduced ECM degradation (Ghosh and Vaughan, 2012; Holm Nielsen et al., 2019; Leask et al., 2002; Leask et al., 2009; Lipson et al., 2012; Omori et al., 2016; Rabieian et al., 2018). PAI-1 and CTGF are associated with virtually all fibrotic pathologies, with CTGF being thought to act cooperatively with TGFβ to sustain fibrosis (Abreu et al., 2002; Lipson et al., 2012; Wang et al., 2011).

The downstream effect of regulating the expression of these genes resulted in changes to ECM synthesis. TGFβ1-stimulated fibroblasts, treated with dHACM, demonstrated decreased type I collagen gene expression, whereas the expression of *COL3A1* remained unchanged. This suggests that dHACM shifts the *COL1A1*-to-*COL3A1* ratio in favor of type-III collagen production. This is a promising outcome because it is similar to the observations made in fetal scarless healing. Early gestation fetal skin contains low levels of TGFβ, resulting in tissue that is virtually devoid of myofibroblasts during cutaneous healing, with type-III collagen predominating (Ma et al., 2015; Moore et al., 2018). After an injury, significant decreases in FN were also observed. FN is another key component of the ECM and plays a vital role in fibrosis through the regulation of the deposition, maturation, and stabilization of other ECM proteins, including type I collagen (Sottile et al., 2007). These data suggest that dHACM regulation of TGFβ signaling can alter ECM synthesis in fibroblasts.

During the fibrotic process, contraction of the deposited ECM components limits mobility and range of motion of the affected tissue (Marshall et al., 2018). This phenomenon occurs as a result of the TGFβ-dependent expression of αSMA stress filaments in myofibroblasts (Van De Water et al., 2013). In the presence of TGFβ1, dHACM treatment decreased gene expression of *αSMA* and additionally prevented stress fiber formation in myofibroblasts. The effects of the dHACM on cellular fibrosis mechanisms were examined in an ex vivo cellular contraction assay. Fibroblasts embedded in a collagen substrate were stimulated with TGFβ1, resulting in significant contraction, ultimately releasing the collagen gel from the surface of the culture plate. When TGFβ1 and dHACM were added simultaneously, dHACM inhibited the TGFβ1-induced contraction proportionate to the dose of treatment. Collectively, these data suggest a potential mechanism by which dHACM regulates myofibroblast activity, reducing abnormal cellular contraction through the regulation of TGFβ-dependent expression of αSMA.

These data provide insight into the effects of dHACM regulation of TGFβ signaling pathways on HDFs and the potential role of dHACM as a modulator of fibrosis. Clinical support for this hypothesis has been shown in an investigation evaluating the benefit of using dHACM in the treatment of pediatric burns. Compared with split-thickness skin grafts, dHACM reduced long-term pain as a result of decreased contractures and reduced overall scarring. The effects of dHACM treatment in in vitro fibrosis models mirrored the benefits observed in these cases (Ahuja et al., 2020). With more than 500,000 patients per year being treated for burns in the United States alone, dHACM may offer a new therapeutic option for patients that would otherwise be left with scars and painful contractures that require major corrective surgery (Asuku et al., 2008; Egeland et al., 2008). Additional studies will be necessary to further explore the processes associated with fibrotic conditions and refine the model by which dHACM is screened as a possible treatment. Preclinical animal models and clinical data will also be beneficial in determining how the in vitro characteristics of dHACM may translate to clinical efficacy in a dynamic system. However, this is an important first step toward understanding the complexities of the regulatory capabilities of dHACM and the targeted pathways for pathologic scar fibrosis.

MATERIALS AND METHODS

Dehydrated human amnion/chorion membrane

dHACM (MiMedx Group) is a dehydrated human allograft comprising laminated amnion and chorion membranes derived from the amniotic sac. Birth tissue was donated under informed written consent, after Cesarean deliveries, in compliance with the Food and Drug Administration's Good Tissue Practice and American Association of Tissue Banks standards. Institutional approval was not required because MiMedx Group is accredited by the American Association of Tissue Banks for donor eligibility assessment, informed consent, acquisition, processing, release, storage, and distribution of birth tissue for transplantation. All donors were tested and confirmed to be free of infectious diseases, including HIV, human T-lymphotropic virus, hepatitis B and C, and syphilis. Amnion and chorion were separated from the placenta and processed following the proprietary PURION process, in which the amnion and chorion layers are gently cleansed, laminated, and dehydrated under controlled conditions.

dHACM extract preparation

To prepare soluble extracts of dHACM for cell culture experiments, individual donors of dHACM were extracted overnight at 40 mg of tissue per milliliter of basal DMEM. Basal media is defined as DMEM (Thermo Fisher Scientific, Waltham, MA) containing 1% penicillin–streptomycin (Thermo Fisher Scientific) and 1% sodium pyruvate (Thermo Fisher Scientific). The tissue residue was removed by centrifugation, and the resultant fluid was passed through a 0.22-μm filter (Millipore Sigma, Burlington, MA). The filtrate was collected in a sterile container to serve as the extract for treatment. Prepared extracts from individual dHACM donors were then diluted in the basal DMEM to the desired testing concentration. Three dHACM donors were used in each subsequent experiment.

Cell culture and treatment

Cryopreserved adult HDFs were purchased from Thermo Fisher Scientific. HDFs between passages 5 and 9 were cultured in DMEM (Thermo Fisher Scientific) containing 10% fetal bovine serum (Thermo Fisher Scientific), 1% penicillin–streptomycin (Fisher Scientific, Waltham, MA), and 1% sodium pyruvate (Thermo Fisher Scientific) at 37 °C and 5% carbon dioxide until 80% confluent. Cells were

detached using TrypLE cell dissociation solution (Thermo Fisher Scientific) and were plated at 25,000 cells/cm^2 for each experiment.

HDFs were pretreated with either basal media or basal media containing 20 ng/ml TGFβ1 (R&D Systems, Minneapolis, MN) for 24 hours. After stimulation, the media were removed, and fresh culture media supplemented with one of the following treatments were added: group #1 basal medium, group #2 TGFβ1, group #3 20 mg/ml dHACM + TGFβ1, group #4 10 mg/ml dHACM + TGFβ1, and group #5 1 mg/ml dHACM + TGFβ1. dHACM extracts were prepared as described earlier (n = 3 dHACM donors). Treatment groups containing dHACM tested individual dHACM donors at the indicated concentrations. All treatment groups were tested with three technical replicates for gene expression and Milliplex analysis and two technical replicates in the cellular contraction assay. For all other analyses, each group was tested individually.

Quantitative PCR

cDNA was prepared utilizing the Cells-2-Ct Kit (Thermo Fisher Scientific), per the manufacturer's instructions. qPCR amplification for each gene target was performed on a QuantStudio 7 Flex Real-Time PCR System (Thermo Fisher Scientific) using predesigned TaqMan Gene Expression Assays for αSMA (Hs00426835_g1), PAI-1 (Hs00167155_m1), CTGF (Hs00170014_m1), COL1A1 (Hs00164004_m1), COL3A1 (Hs00943809_m1), FN1 (Hs01549976_m1), ELN (Hs00355783_m1), and eukaryotic 18s (4319413E) purchased from Thermo Fisher Scientific. Each replicate sample was analyzed in duplicate. The $2^{-\Delta\Delta Ct}$ method was used to determine the relative expression of dHACM-treated HDFs compared with that of TGFβ1-treated HDFs, with eukaryotic 18s as an endogenous control. For graphical representation, the technical replicate values for each dHACM donor were combined.

Western blotting

Proteins were isolated in radioimmunoprecipitation assay buffer (Thermo Fisher Scientific) complemented with a cocktail of protease inhibitors (Millipore Sigma). Cell debris was pelleted by centrifugation at 14,000 r.p.m. at 4 °C for 10 minutes; supernatants were harvested, and protein concentrations were determined with Pierce BCA protein assay (Thermo Fisher Scientific). Equal protein amounts were resolved by 4–12% gradient sodium dodecyl sulfate-polyacrylamide gel electrophoresis and were transferred onto nitrocellulose membranes using iBlot2 device (Thermo Fisher Scientific). Membranes were blocked for 1 hour in 5% nonfat dry milk 1× Tris-buffered saline 0.05% Tween 20 and probed with antibodies against αSMA (Sigma-Aldrich, St. Louis, MO), phosphorylated SMAD2 Ser 465/467 (Cell Signaling Technology, Danvers, MA), SMAD2 (Cell Signaling Technology), or GAPDH (Cell Signaling Technology) overnight at 4 °C. Membranes were washed in 1× Tris-buffered saline 0.05% Tween 20 and incubated with antimouse or antirabbit IgG horseradish peroxidase–conjugated secondary antibodies (Abcam, Cambridge, MA). Immunoreactive proteins were detected using chemiluminescence (Thermo Fisher Scientific) and imaged on the GE Healthcare Imager. Semiquantitative analysis was performed using the ImageJ software (National Institutes of Health) (Schneider et al., 2012). Values for each dHACM donor were combined for graphical representation.

Immunofluorescence

Cells were fixed with 4% paraformaldehyde (Electron Microscopy Science, Hatfield, PA) for 30 minutes at room temperature. Cellular membranes were permeabilized with 0.1% Triton-X-100 for 2 minutes, followed by blocking in Serum-Free Protein Block (Agilent Dako, Santa Clara, CA) for 1 hour at room temperature. Incubation with primary antibody against ascites fluid mouse IgG2a anti human αSMA (Sigma-Aldrich) diluted in Antibody Diluent (Agilent Dako) was carried out overnight at 4 °C. For visualization, cells were incubated with Chicken IgY anti-Mouse IgG (H+L), Alexa Fluor 488 (Thermo Fisher Scientific) and DAPI (Vector Laboratories, Burlingame, CA) to identify the nuclei. Images were acquired on a Leica microscope fitted with ×40 objective using Leica Application Suite Advance Fluorescence software and the THUNDER Imager from Leica (Leica Microsystems, Wetzlar, Germany).

TGFβ signaling pathway Milliplex

Cellular levels of phosphorylated SMAD2 Ser 465/467 were measured using MILLIPLEX Map TGFβ Signaling Pathway Magnetic bead kit (Millipore Sigma). The assay was performed according to the manufacturer's instructions, and Total β-Tubulin Magnetic Bead MAPmates (Millipore Sigma) was used to normalize the data. Each technical replicate was tested in duplicate, and combined values for each dHACM donor were used for graphical representation.

Cell contraction

The effects of dHACM on fibroblast-mediated collagen gel contraction were determined using the Cell Contraction Assay, Floating Matrix (CELL BIOLABS, San Diego, CA), according to the manufacturer's instructions. Briefly, fibroblast-populated collagen gels were created by suspending fibroblasts in a neutralized type-1 collagen solution. The suspended fibroblasts, at a final concentration of 0.2 × 10^6 cells/ml in the collagen solution, were added to each well and incubated at 37 °C for 1 hour to allow for collagen fibril polymerization. Wells containing only collagen solution were used as the negative control. Treatments in a medium containing 1% fetal bovine serum were carefully added to wells and replaced after 24 hours. Treatments include no cells (negative control), media alone (vehicle control), 20 ng/ml TGFβ1 (positive control), 20 mg/ml dHACM + 20 ng/ml TGFβ1, 10 mg/ml dHACM + 20 ng/ml TGFβ1, and 1 mg/ml dHACM + 20 ng/ml TGFβ1. dHACM extracts were prepared as described earlier in basal media containing 1% fetal bovine serum (n = 3 dHACM donors). Each dHACM donor was tested at the indicated concentrations in duplicate. Gel contraction was determined by measuring the gel diameter after 48 hours. Graphical representation combined all values for each dHACM donor.

Collagen gels containing cells were fixed with 4% paraformaldehyde (Electron Microscopy Science) in PBS for 1 hour at 37 °C. Cells were washed in PBS followed by 10 minutes in ice-cold methanol and were then washed in PBS. Fixed gels were blocked in Serum-Free Protein Block (Agilent Dako) for 1 hour at room temperature, followed by incubation with ascites fluid mouse IgG2a anti human αSMA (Sigma-Aldrich) in Antibody Diluent (Agilent Dako) at 4 °C overnight. For visualization, collagen gels were incubated with Chicken IgY anti-Mouse IgG (H+L), Alexa Fluor 488 (Thermo Fisher Scientific) and DAPI (Thermo Fisher Scientific) to identify the nuclei. Control staining included Mouse IgG2a (Thermo Fisher Scientific) and secondary antibodies only. Images were acquired on a Leica microscope fitted with ×20 objective using Leica Application Suite Advance Fluorescence software (Leica Microsystems).

Statistical analysis

All values are reported as mean ± SD, and statistical analyses were performed using GraphPad Prism software. All data were compared with those of the TGFβ1 and media alone group within each experiment using a one-way ANOVA. For each ANOVA, pairwise

comparisons were made using a Tukey test. A significant difference was assigned when $P < 0.05$.

Data availability statement

No datasets were generated or analyzed during this study.

ORCIDs

Sarah E. Moreno: https://orcid.org/0000-0002-6726-7223
Michelle Massee: https://orcid.org/0000-0001-9025-0879
Thomas J. Koob: https://orcid.org/0000-0001-6162-4202

AUTHOR CONTRIBUTIONS

Formal Analysis: SEM; Investigation: SEM; Methodology: SEM, MM; Resources: SEM; Supervision: MM, TJK; Writing - Original Draft Preparation: SEM, MM; Writing - Review and Editing: SEM, MM, TJK

ACKNOWLEDGMENTS

This study was sponsored and funded by MiMedx Group.

CONFLICT OF INTEREST

All authors are employees of MiMedx Group. All authors hold equity in MiMedx Group.

REFERENCES

Abreu JG, Ketpura NI, Reversade B, De Robertis EM. Connective-tissue growth factor (CTGF) modulates cell signalling by BMP and TGF-beta. Nat Cell Biol 2002;4:599–604.

Ahuja N, Jin R, Powers C, Billi A, Bass K. Dehydrated human amnion chorion membrane as treatment for pediatric burns. Adv Wound Care (New Rochelle) 2020;9:602–11.

Asuku M, Ibrahim A, Ijekeye FO. Post-burn axillary contractures in pediatric patients: a retrospective survey of management and outcome. Burns 2008;34:1190–5.

Brown BC, McKenna SP, Siddhi K, McGrouther DA, Bayat A. The hidden cost of skin scars: quality of life after skin scarring. J Plast Reconstr Aesthet Surg 2008;61:1049–58.

Cazzell S, Stewart J, Agnew PS, Senatore J, Walters J, Murdoch D, et al. Randomized controlled trial of micronized dehydrated human amnion/chorion membrane (dHACM) injection compared to placebo for the treatment of plantar fasciitis. Foot Ankle Int 2018;39:1151–61.

Egeland B, More S, Buchman SR, Cederna PS. Management of difficult pediatric facial burns: reconstruction of burn-related lower eyelid ectropion and perioral contractures. J Craniofac Surg 2008;19:960–9.

El Ayadi A, Jay JW, Prasai A. Current approaches targeting the wound healing phases to attenuate fibrosis and scarring. Int J Mol Sci 2020;21:1105.

Fetterolf DE, Snyder RJ. Scientific and clinical support for the use of dehydrated amniotic membrane in wound management. Wounds 2012;24:299–307.

Frangogiannis N. Transforming growth factor-β in tissue fibrosis. J Exp Med 2020;217:e20190103.

Gauglitz GG, Korting HC, Pavicic T, Ruzicka T, Jeschke MG. Hypertrophic scarring and keloids: pathomechanisms and current and emerging treatment strategies. Mol Med 2011;17:113–25.

Ghosh AK, Vaughan DE. PAI-1 in tissue fibrosis. J Cell Physiol 2012;227:493–507.

Györfi AH, Matei AE, Distler JHW. Targeting TGF-β signaling for the treatment of fibrosis. Matrix Biol 2018;68–69:8–27.

Holm Nielsen S, Willumsen N, Leeming DJ, Daniels SJ, Brix S, Karsdal MA, et al. Serological assessment of activated fibroblasts by alpha-smooth muscle actin (α-SMA): a noninvasive biomarker of activated fibroblasts in lung disorders. Transl Oncol 2019;12:368–74.

Koob TJ, Rennert R, Zabek N, Massee M, Lim JJ, Temenoff JS, et al. Biological properties of dehydrated human amnion/chorion composite graft: implications for chronic wound healing. Int Wound J 2013;10:493–500.

Koob TJ, Lim JJ, Massee M, Zabek N, Denozière G. Properties of dehydrated human amnion/chorion composite grafts: implications for wound repair and soft tissue regeneration. J Biomed Mater Res B Appl Biomater 2014a;102:1353–62.

Koob TJ, Lim JJ, Massee M, Zabek N, Rennert R, Gurtner G, et al. Angiogenic properties of dehydrated human amnion/chorion allografts: therapeutic potential for soft tissue repair and regeneration. Vasc Cell 2014b;6:10.

Leask A, Holmes A, Abraham DJ. Connective tissue growth factor: a new and important player in the pathogenesis of fibrosis. Curr Rheumatol Rep 2002;4:136–42.

Leask A, Parapuram SK, Shi-Wen X, Abraham DJ. Connective tissue growth factor (CTGF, CCN2) gene regulation: a potent clinical bio-marker of fibroproliferative disease? J Cell Commun Signal 2009;3:89–94.

Lei J, Priddy LB, Lim JJ, Massee M, Koob TJ. Identification of extracellular matrix components and biological factors in micronized dehydrated human amnion/chorion membrane. Adv Wound Care (New Rochelle) 2017;6:43–53.

Lipson KE, Wong C, Teng Y, Spong S. CTGF is a central mediator of tissue remodeling and fibrosis and its inhibition can reverse the process of fibrosis. Fibrogenesis Tissue Repair 2012;5(Suppl. 1):S24.

Ma X, Yang F, Yang S, Rasul A, Li T, Liu L, et al. Number and distribution of myofibroblasts and α-smooth muscle actin expression levels in fetal membranes with and without gestational complications. Mol Med Rep 2015;12:2784–92.

Marshall CD, Hu MS, Leavitt T, Barnes LA, Lorenz HP, Longaker MT. Cutaneous scarring: basic science, current treatments, and future directions. Adv Wound Care (New Rochelle) 2018;7:29–45.

Massee M, Chinn K, Lei J, Lim JJ, Young CS, Koob TJ. Dehydrated human amnion/chorion membrane regulates stem cell activity in vitro. J Biomed Mater Res B Appl Biomater 2016a;104:1495–503.

Massee M, Chinn K, Lim JJ, Godwin L, Young CS, Koob TJ. Type I and II diabetic adipose-derived stem cells respond in vitro to dehydrated human amnion/chorion membrane allograft treatment by increasing proliferation, migration, and altering cytokine secretion. Adv Wound Care (New Rochelle) 2016b;5:43–54.

Moore AL, Marshall CD, Barnes LA, Murphy MP, Ransom RC, Longaker MT. Scarless wound healing: transitioning from fetal research to regenerative healing. Wiley Interdiscip Rev Dev Biol 2018;7:e309.

Omori K, Hattori N, Senoo T, Takayama Y, Masuda T, Nakashima T, et al. Inhibition of plasminogen activator inhibitor-1 attenuates transforming growth factor-β-dependent epithelial mesenchymal transition and differentiation of fibroblasts to myofibroblasts. PLoS One 2016;11:e0148969.

Patel VR, Samavedi S, Bates AS, Kumar A, Coelho R, Rocco B, et al. Dehydrated human amnion/chorion membrane allograft nerve wrap around the prostatic neurovascular bundle accelerates early return to continence and potency following robot-assisted radical prostatectomy: propensity score-matched analysis. Eur Urol 2015;67:977–80.

Price DT, Price TC. Robotic repair of a vesicovaginal fistula in an irradiated field using a dehydrated amniotic allograft as an interposition patch. J Robot Surg 2016;10:77–80.

Rabieian R, Boshtam M, Zareei M, Kouhpayeh S, Masoudifar A, Mirzaei H. Plasminogen activator inhibitor type-1 as a regulator of fibrosis. J Cell Biochem 2018;119:17–27.

Schneider CA, Rasband WS, Eliceiri KW. NIH Image to ImageJ: 25 years of image analysis. Nat Methods 2012;9:671–5.

Serena TE, Carter MJ, Le LT, Sabo MJ, DiMarco DT, EpiFix VLU Study Group. A multicenter, randomized, controlled clinical trial evaluating the use of dehydrated human amnion/chorion membrane allografts and multilayer compression therapy vs. multilayer compression therapy alone in the treatment of venous leg ulcers. Wound Repair Regen 2014;22:688–93.

Sottile J, Shi F, Rublyevska I, Chiang HY, Lust J, Chandler J. Fibronectin-dependent collagen I deposition modulates the cell response to fibronectin. Am J Physiol Cell Physiol 2007;293:C1934–46.

Vallée A, Lecarpentier Y. TGF-β in fibrosis by acting as a conductor for contractile properties of myofibroblasts. Cell Biosci 2019;9:98.

Van De Water L, Varney S, Tomasek JJ. Mechanoregulation of the myofibroblast in wound contraction, scarring, and fibrosis: opportunities for new therapeutic intervention. Adv Wound Care (New Rochelle) 2013;2:122–41.

Walton KL, Johnson KE, Harrison CA. Targeting TGF-β mediated SMAD signaling for the prevention of fibrosis. Front Pharmacol 2017;8:461.

Wang Q, Usinger W, Nichols B, Gray J, Xu L, Seeley TW, et al. Cooperative interaction of CTGF and TGF-β in animal models of fibrotic disease. Fibrogenesis Tissue Repair 2011;4:4.

Wynn TA. Cellular and molecular mechanisms of fibrosis. J Pathol 2008;214:199–210.

Yazdani S, Bansal R, Prakash J. Drug targeting to myofibroblasts: implications for fibrosis and cancer. Adv Drug Deliv Rev 2017;121:101–16.

Zelen CM, Serena TE, Denoziere G, Fetterolf DE. A prospective randomised comparative parallel study of amniotic membrane wound graft in the management of diabetic foot ulcers. Int Wound J 2013;10:502–7.